



ELSEVIER

Physica B 324 (2002) 254–260

PHYSICA B

www.elsevier.com/locate/physb

# Observation of mixed two-phase state in $\text{Eu}_{0.7}\text{Pb}_{0.3}\text{MnO}_3$ single crystal by magnetic resonance method

N.V. Volkov\*, G.A. Petrakovskii, V.N. Vasiliev, D.A. Velikanov, K.A. Sablina, K.G. Patrin

*L.V. Kirensky Institute of Physics SB RAS, Krasnoyarsk 660036, Russia*

Received 16 May 2002; accepted 18 July 2002

## Abstract

The magnetic resonance measurements show that the mixed two-phase state takes place in the  $\text{Eu}_{0.7}\text{Pb}_{0.3}\text{MnO}_3$  single crystal. The coexistence of the magnetic phases is observed in vicinity of the magnetic phase transition, where the sample exhibits the effect of the CMR. The frequency-field dependencies of the spectra allow to conclude that these phases are paramagnetic and ferromagnetic ones. Moreover, the study of the frequency dependencies shows the sensitivity of the mixed-phase state to the external magnetic field. This suggests that the scenario of the phase separation is realized in this case and the mixed two-phase state is not related to simple chemical inhomogeneity.

© 2002 Elsevier Science B.V. All rights reserved.

PACS: 76.50.+g; 72.20.My

Keywords: Manganites; CMR; Magnetic resonance; Phase separation

## 1. Introduction

Manganese oxides with the perovskite structure of the  $\text{M}_x\text{A}_{1-x}\text{MnO}_3$  ( $\text{M}=\text{La}, \text{Pr}, \text{Nd}, \text{Eu}, \dots$ ,  $\text{A}=\text{Ca}, \text{Sr}, \text{Pb}, \dots$ ) family, widely known as “manganites”, have attracted considerable attention as the system with strongly correlated electrons. Due to the presence of strong coupling of the spin, charge and orbital subsystems the manganites reveal a very rich ( $x, H, T$ )-phase diagram with antiferromagnetic, metallic or insulating ferromagnetic, charge and orbital ordered

regions [1]. This richness is due to competition between a variety of the interactions with very similar energy scales. The energy balance can be so delicate that question of the ground state of the system is subtle. Many have suggested that the ground state in this case can be inhomogeneous. Presently a variety of experimental studies of the doped manganites support the existence of the phase separation picture in the vicinity of the magnetic ordering temperature. Considerable progress has been achieved in the theoretical analysis of the mixed-phase tendencies in these compounds [2]. However, a full understanding of the phase separation phenomenon and its role in origin of the CMR and other interesting effects is still lacking. This circumstance earnestly requires

\*Corresponding author. Tel.: +73912-430763; fax: +73912-438923.

E-mail address: volk@iph.krasn.ru (N.V. Volkov).

extending the search both of new materials with the phase separation and new experimental techniques for its investigations.

The phase-separation scenarios discussed at present for manganites suppose the different magnetic state of the coexisted phase, so the electron magnetic resonance method can be an effective tool for probing the inhomogeneities in the samples. The magnetic resonance has been extensively used for studying the doped manganites (for example, [3–6]). The studies mainly are limited by the paramagnetic region (above the Curie temperature  $T_C$ ). However, the works carried out by several groups using magnetic resonance technique in a wide temperature range show that the magnetic mixed-phase state is realized in the vicinity of  $T_C$  [7–11]. But the systematical investigation of the  $M_xA_{1-x}MnO_3$  crystals near  $T_C$  is lacking. In this work, we used the magnetic resonance method for probing the inhomogeneity of the  $Eu_{0.7}Pb_{0.3}MnO_3$  single crystal.

## 2. Experimental techniques

The single crystals of  $Eu_{0.7}Pb_{0.3}MnO_3$  were grown by a method of spontaneous crystallization from solution in a melt. The choice of the Pb ions was dictated by the peculiarity of the technology, the mixture of PbO and  $PbF_2$  was used as the solvent and at the same time it provided the plumbum content in the crystals. One of the reasons as to why we have focused on the Eu-containing manganite materials is that the ions reveal mixed valency in oxides ( $Eu^{2+}$ ,  $Eu^{3+}$ ) and earlier the combination of the Eu and Pb ions in the manganite did not occur in the literature. X-ray analyses confirmed the composition of the crystals and showed that the samples are single-phase perovskites. All measurements were carried out on well-polished plate-like samples of the size of about  $2 \times 2 \times 0.1 \text{ mm}^3$ .

The magnetic resonance measurements were performed with both a conventional cavity perturbation technique with microwave frequency  $\nu = 25 \text{ GHz}$  and with a spectrometer operating in  $\nu = 37\text{--}80 \text{ GHz}$  frequency range with a pulsed

external magnetic field of 0–40 kOe. The magnetization data were acquired by SQUID magnetometer. The magnetoresistance was measured by the standard four-probe technique with external magnetic field up to 12 kOe.

## 3. Experimental results and discussion

Using conventional scheme of the spectrometer at 25 GHz with field modulation the spectra was recorded as derivatives of the absorption lines. It was observed that spectra having smooth shape at high temperatures reveal a structure in temperature range from 240 to 140 K. Below  $T \sim 140 \text{ K}$  the structure in the resonance spectra vanished again. For detailed analysis we integrated the experimental spectra and applied a fitting procedure by Lorentzian lines. Fig. 1 shows that the observed spectra could be fitted satisfactorily, only if we assumed the presence of two lines. The dashed lines show best results of the two-Lorentzian lines analysis for the absorption lines at various temperatures. At temperatures above  $T \sim 240 \text{ K}$  the absorption line is fitted well by single-Lorentzian line. When the temperature decreases further, coexistence of two signals takes place. At temperatures below 140 K the absorption line has a strongly asymmetric shape that complicates the analysis. This line asymmetry is caused by abrupt increasing of the sample conductivity (Fig. 2a). When a skin depth  $\delta = (\rho/\mu_0\omega)^{1/2}$  becomes comparable to or smaller than the sample thickness, the electric and magnetic microwave components are out of phase in the sample. This leads to an admixture of a dispersion into absorption spectra and the line acquires Dysonian-like shape [12,13]. Really, the magnetic resonance absorption line recorded at  $T = 120 \text{ K}$  does not exhibit any structure and fits well by proper combination of the absorptive and dispersive part of the single-Lorentzian line.

Our primary interest was the temperature dependencies of the integrated intensities of two coexisting lines in the spectra (Fig. 2b). Assuming that two lines in the spectra are the magnetic resonance absorption from paramagnetic (PM) and ferromagnetic (FM) regions in the sample (the

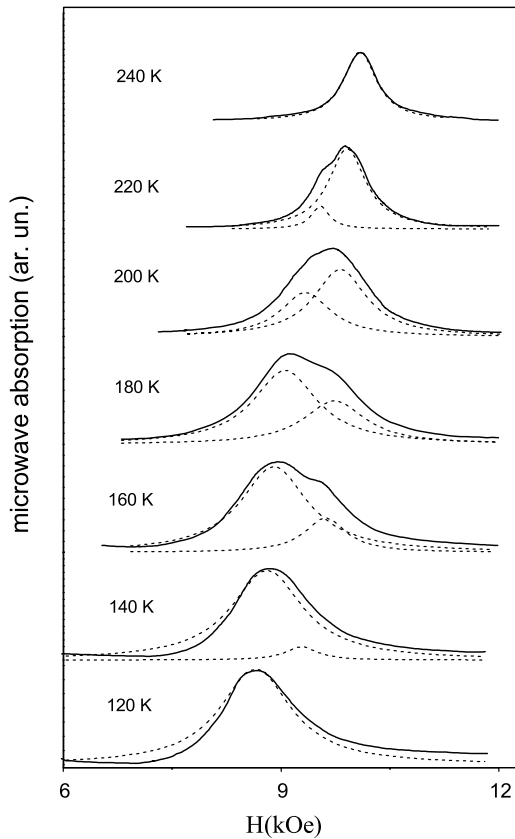


Fig. 1. Magnetic resonance spectra at various temperatures. Solid lines are the experimental absorption lines, dashed lines are the best fitting by two-Lorentzian lines.

confirmation for this will be given below), the line intensity dependencies illustrate an evolution of the mixed two-phase state with temperature and magnetic field. At  $T \sim 300$  K the crystal is in homogeneous PM state and only single PM absorption line is observed in the spectra. The intensity of the PM resonance line  $I_{PM}$  follows reasonably well the temperature dependence of a paramagnetic susceptibility  $\chi_{DC}$ , which strongly increases when the temperature approaches  $T_C$  from above. Fig. 3 shows that an inverse susceptibilities  $1/\chi_{DC}$  and  $1/I_{PM}$  versus  $T$  behave linearly according to Curie–Weiss law  $\chi_{DC}^{-1} \sim (T - \theta_{CW})$  within the temperature range from 300 K to about 235 K. A linear extrapolation for both dependencies gives the Curie–Weiss temperature  $\theta_{CW} \approx 210$  K, which coincides with  $T_C$  determined

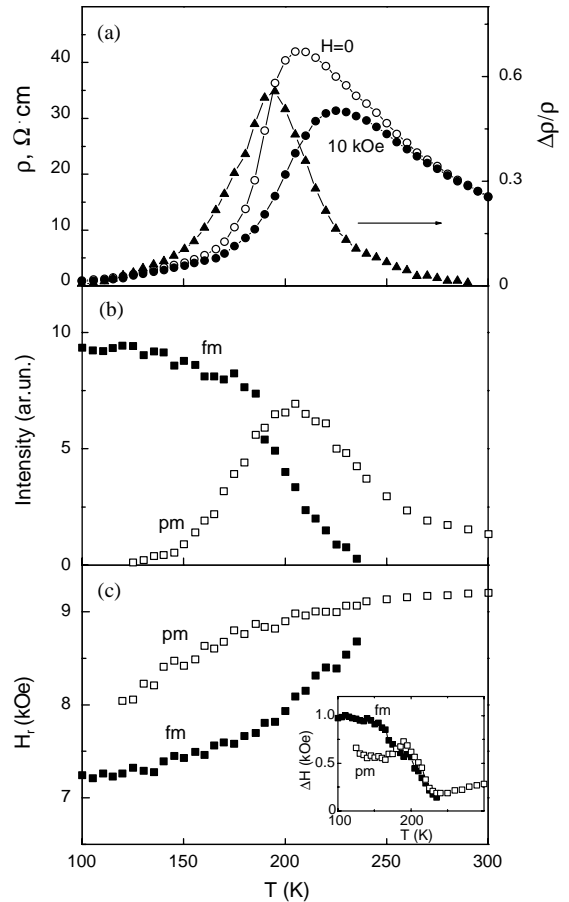


Fig. 2. (a) Temperature dependence of the resistivity  $\rho$  and magnetic resistance  $\Delta\rho/\rho(0)$  (a); Temperature dependencies of the paramagnetic (PM) and ferromagnetic (FM) line parameters ( $\nu = 25$  GHz): (b) intensity, (c) resonance field, and (inset) line width.

from low-field magnetization data in the inset Fig. 3. The similar temperature dependencies for the  $I_{PM}$  and  $\chi_{DC}$  clearly indicate that all the Mn ions contribute to the observed spectra. For temperatures below 235 K the curve for the inverse susceptibility  $1/\chi_{DC}$  versus  $T$  shows the positive curvature suggesting spin clustering effects [14]. In our case the line corresponding to ferromagnetic resonance absorption in the spectra appears at the same temperature  $T \sim 235$  K, which is above  $T_C$ . As the temperature is lowered further, the concentration of the FM phase in the sample increases and apparently  $T_C$  is the temperature for which a percolation threshold on the

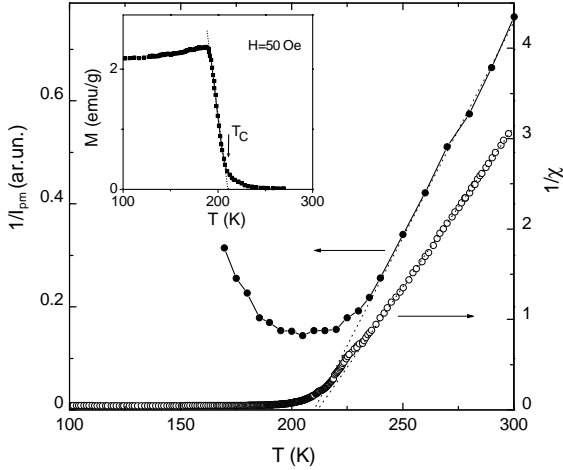


Fig. 3. Inverse magnetic susceptibility  $1/\chi_{DC}$  and inverse intensity of the paramagnetic absorption line  $1/I_{PM}$  versus temperature. Insert: the magnetization data for the sample as function of temperature at  $H = 50$  Oe.

FM/conducting regions takes place. A change of type of the conductivity at  $T_C$  confirms this assumption (Fig. 2a). Below  $T \sim 120$  K the whole sample is in the FM state.

Fig. 2b shows the temperature behavior of the PM and FM line intensities ( $I_{PM}$  and  $I_{FM}$ , respectively), which reflects the change of the ratio of the PM and FM phase volumes in the sample with temperature. Note, however that it is not only the phase volumes, which make contribution to the line intensities. So we concluded above that  $I_{PM}$  is proportional to  $\chi_{DC}$  and consequently the following expression can be written:

$$I_{PM} \sim V_{PM}(H, T) \cdot \chi_{PM}(H, T), \quad (1)$$

where  $V_{PM}(H, T)$  is the volume of the PM phase. For the  $I_{FM}$  we can assume that

$$I_{FM} \sim V_{FM}(H, T) \cdot M_{FM}(H, T), \quad (2)$$

here,  $V_{FM}(H, T)$  and  $M_{FM}(H, T)$  are the volume and the magnetization of the FM phase, respectively.

Fig. 2c shows the temperature dependencies of the resonance fields ( $H_r^{FM}$  and  $H_r^{PM}$ ) and line widths ( $\Delta H_{FM}$  and  $\Delta H_{PM}$ ) for the FM and PM lines in the magnetic resonance spectra. We will not discuss in detail the behavior of these parameters but only make some remarks. The

different mechanisms describing the observed great broadening of the  $\Delta H_{FM}$  and  $\Delta H_{PM}$  below  $T_C$  can be considered and such questions have been discussed widely in literature. The nature of the broadening can be determined by the magnetic inhomogeneity (that is obviously observed), the quality and shape of the crystals, which determine the contribution of the demagnetizing field energy in the Hamiltonian of the system. The essential effect on the line width can be caused by the relaxation process related to magnon scattering on charge carriers. The role of these processes increases at increasing the conductivity of the samples. The Jahn–Teller dynamical effect can cause the broadening of the resonance line too [5].

The shift of the resonance field to lower fields for absorption line corresponding to the FM phase  $H_r^{FM}$  is attributed to increasing the magnetization of the sample. Our samples may be approximated by infinite plate and so the expression for  $H_r^{FM}$  can be written as

$$\frac{\omega}{\gamma} = (H_r^{FM}(H_r^{FM} + 4\pi M_{FM}^*))^{1/2}, \quad (3)$$

here,  $\omega = 2\pi\nu$  is a cyclic frequency,  $\gamma$  is a gyromagnetic ratio,  $M_{FM}^*$  is an effective magnetization, which may differ from  $M_{FM}$  due to influence of the magnetic anisotropy and the magnetic crystal inhomogeneity. The magnetic anisotropy of the 3D perovskite-like manganites is generally small. In our case, studying the samples of a spherical shape we observed that one is no more than 120 Oe at  $T = 100$  K. The magnetic inhomogeneity of the samples results in the demagnetizing effect. Thus, the internal magnetic field within sample must be corrected by a demagnetizing field. But principal values determining the angular variations of the resonance field cannot be exactly calculated for general case. At the same time, the results obtained by Geschwind and Clogston can be used for evaluation [15]. They concluded that the variation of the internal magnetic field may be in a range up to  $2\pi M_{FM}$ .

The PM line shifts to lower field as  $T$  decreases from  $T_C$ . This can be explained either by the influence of the demagnetizing fields from the FM regions or by the change of the  $g$ -factor which

takes place as a result of the Jahn–Teller distortions at  $T < T_C$ . It should be noted that in the case of  $\text{La}_{0.7}\text{Pb}_{0.3}\text{MnO}_3$  [10], we did not observe the shift of the resonance field of PM line with the exception of a small increase of one at  $T \sim T_C$ .

When the inhomogeneous state is observed in the system, there appear questions concerning the magnetic and electronic states of the coexisting phases and origin of the inhomogeneity in the system. One of the mechanisms leading to the two-phase magnetic state is simply the chemical inhomogeneity of the crystals composition. In this case the regions with different  $T_C$  occur in the sample volume, so the PM and FM phases can coexist in the temperature interval determined by a dispersion of the transition temperature  $T_C$ . Moreover, two models of the phase separation for the manganites have been discussed recently. There are (i) electronic phase separation between phases with different densities that leads to nanometer scale coexisting FM/conducting and PM (or antiferromagnetic)/insulating clusters [16], and (ii) disorder-induced phase separation on the FM/conducting and PM/insulating regions with equal carrier density [17,18]. The coexisting phases in the latter can be as large as a micrometer in size.

The study of the field-frequency dependencies of the magnetic resonance spectra is a very powerful method to determine the magnetic state of the system and its behavior in the external magnetic field. At first we have applied this method for the study of the mixed two-phase state in the  $\text{La}_{0.7}\text{Pb}_{0.3}\text{MnO}_3$  single crystal [10]. Fig. 4 shows the field-frequency dependencies for two observed lines in the magnetic resonance spectra of the  $\text{Eu}_{0.7}\text{Pb}_{0.3}\text{MnO}_3$  at  $T = 205$  K. It is expected that the dependence for FM line will follow expression (2). Since at  $T = 205$  K the sample is far from the magnetic saturation we must take into consideration the dependence of  $M_{\text{FM}}^*$  on the temperature. To fit the experimental data we suppose that  $M_{\text{FM}}^*(H)$  and  $M_{\text{FM}}(H)$  do not strongly differ from each other, and Brillouin function for the  $M_{\text{FM}}(H)$  was used:

$$M_{\text{FM}} = M_0 B_S \left( \frac{3T_C S}{k_B T} \left( \frac{g\mu_B(S+1)}{3k_B T_C} H + \frac{M_{\text{FM}}}{M_0} \right) \right), \quad (4)$$

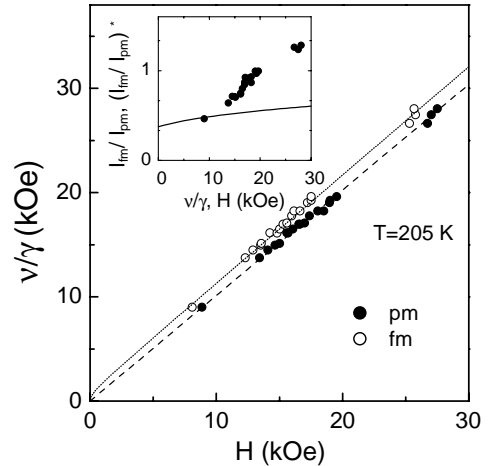


Fig. 4. Frequency-field dependencies of the PM and FM absorption lines observed in the magnetic resonance spectrum at 205 K. Dotted lines are extrapolations of experimental points by the dependencies (3) and (5) (see text). Inset: the ratio of the intensities of the ferromagnetic and paramagnetic lines ( $I_{\text{FM}}/I_{\text{PM}}$ ) versus microwave frequency; solid line represent dependence ( $I_{\text{FM}}/I_{\text{PM}}$ )<sup>\*</sup> (see text) as function of magnetic field.

here,  $M_0$  is the saturation magnetization,  $S = 2(1-x) + 3x/2$  and  $x = 0.3$ . The result of fitting is shown in Fig. 4 by dotted line for  $M_{\text{FM}}(H, T) = 0.15$  at  $T = 205$  K and  $H = 0$ .

For the PM regions the demagnetising effect can be neglected as the magnetization is small and expected frequency-field dependency for the PM resonance line can be described by the expression  $\omega/\gamma = H_{\text{r}}^{\text{PM}}$ . However, it turned out that the experimental data are well fitted by the following equation:

$$\frac{\omega}{\gamma} = H_{\text{r}}^{\text{PM}} + H_{\text{eff}}, \quad (5)$$

where, the external magnetic field  $H$  for the PM regions is corrected by the effective field  $H_{\text{eff}}$ , which depends on  $H$ . The dependence of the  $H_{\text{eff}}$  on  $H$  has behavior similar to  $M_{\text{FM}}(H)$  (see Eq. (4)), which has been used for approximation of the frequency-field dependence for FM line. The value of the  $H_{\text{eff}}$  amounts to  $\sim 15\%$  of the  $4\pi M_{\text{FM}}(H)$  value. This suggests such kind of the mixed-phase picture in the crystal, where the PM regions are located in the demagnetizing field from FM regions. Further support for this

conclusion is the temperature dependence of the  $H_r^{\text{PM}}$  below  $T_C$  (see Fig. 2c). With decreasing temperature, the magnetization and volume of the FM phase in the sample grow, which leads to an increase of the demagnetizing field. As a result, the resonance field  $H_r^{\text{PM}}$  shifts to the low fields.

It is interesting to notice that with microwave frequency (or the magnetic field) increasing the relative intensity of the FM line  $I_{\text{FM}}$  increases, on the contrary, PM line intensity  $I_{\text{PM}}$  decreases. This result is shown in inset of Fig. 4, where the ratio  $I_{\text{FM}}/I_{\text{PM}}$  as a function microwave frequency is plotted. The observed behavior of the  $I_{\text{FM}}/I_{\text{PM}}$  can not be explained only by the increase of  $M_{\text{FM}}(H)$ . For comparison in inset of Fig. 4 we plotted the dependence  $(I_{\text{FM}}/I_{\text{PM}})^*$  as a function of the  $H$ , here we supposed that  $I_{\text{PM}}$  and  $I_{\text{FM}}$  are expressed by Eqs. (1) and (2) respectively but the volumes of the PM and FM phases are constants. Moreover, it was supposed for simplicity that  $\chi_{\text{PM}}$  is independent on the  $H$  too, thus  $(I_{\text{FM}}/I_{\text{PM}})^*$  can be written in the form  $(I_{\text{FM}}/I_{\text{PM}})^* = CM_{\text{FM}}$ , where  $M_{\text{FM}}$  is the FM magnetization obtained in the molecular field approximation (Eq. (4)). For pictorial view we set the constant  $C$  so that  $(I_{\text{FM}}/I_{\text{PM}})^*$  coincides with ratio  $(I_{\text{FM}}/I_{\text{PM}})$  obtained from the experimental spectrum at microwave frequency  $\nu = 25$  GHz. As seen in inset of Fig. 4 the  $(I_{\text{FM}}/I_{\text{PM}})$  grows more rapidly with increasing the magnetic field, than  $(I_{\text{FM}}/I_{\text{PM}})^*$ . This observation suggests that the magnetic field changes the phase state of the sample, as  $H$  increases, the volume of FM phase  $V_{\text{FM}}(H, T)$  in the sample grows but the volume of the PM phase  $V_{\text{PM}}(H, T)$  is reduced. This mechanism leads to observed growth of the ratio  $(I_{\text{FM}}/I_{\text{PM}})$ . One can notice that the above results confirm the picture of the phase separation in the sample because the strong effect of the external magnetic field can hardly be expected in the case when the chemical inhomogeneity of the sample takes place.

Thus, the magnetic resonance measurements show that the mixed two-phase state takes place in the  $\text{Eu}_{0.7}\text{Pb}_{0.3}\text{MnO}_3$  single crystals. The coexistence of PM and FM phases is observed in vicinity of the magnetic phase transition, where the sample exhibits the effect of a colossal magnetic resistance. The main feature of our resonance

investigation is the study of the spectrum parameters as function of the microwave irradiation frequency. This method is found to be a very powerful technique for the determination of the magnetic states of the coexisting phases. The frequency-field dependencies of the spectra allow to conclude that these phases are PM and FM ones. Moreover the study of the frequency dependencies is an effective tool for probing the sensitivity of the mixed-phase state to the external magnetic field. We have established that ratio of FM and PM line intensities increases more rapidly at increasing  $H$ , than the magnetization of the FM regions in the crystal. The result can be explained by the growth of the FM phase with the increase of  $H$ . This leads us to the conclusion that the scenario of the phase separation is realized in this case and mixed two-phase state is not related to simple chemical inhomogeneity.

The picture of the FM/conducting and PM/insulating phase coexistence suggests that the change of the conductivity type in  $\text{Eu}_{0.7}\text{Pb}_{0.3}\text{MnO}_3$  manifests the percolation-like character. The FM/conducting regions arise and percolate in the vicinity of the phase transition. The external magnetic field causes the growth of the FM/conducting regions changing the percolation threshold, as a result the CMR effect is observed. It is interesting that for this case the paramagnetic-ferromagnetic phase transition can be a first-order in character [19]. Really, in our case all experimental temperature dependencies including the resistivity, magnetization and parameters of the magnetic resonance spectra have a hysteresis on cooling and heating.

#### 4. Conclusion

In summary, results shown above provide one more experimental evidence for inhomogeneities in the manganites. The sensitivity of the inhomogeneous state to applied magnetic field suggests that one of the phase separation scenarios is realized in our case. In conclusion, the magnetic resonance methods including both the conventional technique and the scheme of spectrometer with the microwave frequency tuning are found to be the

powerful instruments for probing the magnetic inhomogeneity in the manganite single crystals.

### Acknowledgements

This work was supported by KRSF-RFBR “Enisey2002” Grant No. 02-02-97702. Authors thank Dr. G.V. Bondarenko for performing X-ray analysis of the experimental samples.

### References

- [1] J.S. Zhou, J.B. Goodenough, *Phys. Rev. Lett.* 80 (1998) 2665.
- [2] E. Dagotto, T. Hotta, A. Moreo, *Phys. Rep.* 344 (2001) 1.
- [3] M.S. Seehra, M.M. Ibrahim, V.S. Baby, G. Srinivasan, *J. Phys.: Condens. Matter* 8 (1996) 11283.
- [4] D.L. Huber, G. Alejandro, A. Caneiro, M.T. Causa, F. Prado, M. Tovar, S.B. Oseroff, *Phys. Rev. B* 60 (12) (1999) 155.
- [5] A. Shengelaya, G. Zhao, H. Keller, K.A. Muller, B.I. Kochelaev, *Phys. Rev. B* 61 (2000) 5888.
- [6] F. Rivadulla, M.A. Lopez-Quintela, L.E. Hueso, J. Rivas, M.T. Causa, C. Ramos, R.D. Sanchez, M. Tovar, *Phys. Rev. B* 60 (11) (1999) 922.
- [7] A.K. Srivastava, C.M. Srivastava, R. Mahesh, C.N.R. Rao, *Solid State Comm.* 99 (1996) 161.
- [8] S.L. Yuan, J.Q. Li, Y.P. Yang, X.Y. Zeng, G. Li, F. Tu, G.Q. Zhang, C.Q. Tang, S.Z. Jin, *Phys. Rev. B* 62 (2000) 5313.
- [9] V.A. Atsarkin, V.V. Demidov, G.A. Vasneva, K. Conder, *Phys. Rev. B* 63 (2001) 092405.
- [10] G.A. Petrakovskii, N.V. Volkov, V.N. Vasil’ev, K.A. Sablina, *JETP Lett.* 71 (4) (2000) 144.
- [11] A.I. Shames, E. Rozenberg, W.H. McCarroll, M. Greenblatt, G. Gorodetsky, *Phys. Rev. B* 64 (2001) 172401.
- [12] F. Rivadulla, L.E. Hueso, Lopez-Quintela, J., Rivas, M.T. Causa, *Phys. Rev. B* 64 (2001) 106401.
- [13] M. Peter, B. Shaltiel, J.H. Wenick, H.J. Williams, J.B. Mock, R. Sherwood, *Phys. Rev.* 126 (1962) 1395.
- [14] M. Jaime, P. Lin, S. Chun, M. Salomon, *Phys. Rev. B* 60 (1999) 1028.
- [15] S. Geschwind, A. Clogston, *Phys. Rev.* 108 (1957) 49.
- [16] E.L. Nagaev, *Phys. Usp.* 41 (1998) 831.
- [17] M. Fath, S. Freisem, A.A. Menovsky, et al., *Science* 285 (1999) 1540.
- [18] M. Uehara, S. Mori, C.H. Chen, S.-W. Cheong, *Nature* 399 (1999) 560.
- [19] M. Salamon, M. Jaime, *Rev. Mod. Phys.* 73 (2001) 583.